Self-Healing Resilient Distribution Systems Based on Sectionalization Into Microgrids

Zhaoyu Wang, *Student Member, IEEE*, and Jianhui Wang, *Senior Member, IEEE*

***Abstract*—This paper proposes a novel comprehensive operation and self-healing strategy for a distribution system with both dispatchable and nondispatchable distributed generators (DGs). In the normal operation mode, the control objective of the system is to minimize the operation costs and maximize the revenues. A rolling-horizon optimization method is used to schedule the outputs of dispatchable DGs based on forecasts. In the self-healing mode, the on-outage portion of the distribution system will be optimally sectionalized into networked self-supplied microgrids (MGs) so as to provide reliable power supply to the maximum loads continuously. The outputs of the dispatchable DGs will be rescheduled accordingly too. In order to take into account the uncertainties of DG outputs and load consumptions, we formulate the problems as a stochastic program. A scenario reduction method is applied to achieve a tradeoff between the accuracy of the solution and the computational burden. A modified IEEE 123-node distribution system is used as a test system. The results of case studies demonstrate the effectiveness of the proposed methodology.**

***Index Terms*—Distributed power generation, microgrid (MG), power distribution, power distribution faults, self-healing, stochastic optimization.**

NOMENCLATURE

A. Sets

I	Set of nodes in unfaulted area.
K	Set of nodes in on-outage area.
S	Set of scenarios.
N	Set of types of renewable energy source (RES)-based DGs (wind and solar in this paper) $N = WT, PV$.

B. Acronyms

WT	Wind turbine.
PV	Photovoltaic generator.
MT	Micro turbine.
MG	Microgrid.

Manuscript received April 27, 2014; revised August 13, 2014 and October 29, 2014; accepted November 02, 2014. The work of J. Wang was supported by the U.S. Department of Energy Office of Electricity Delivery and Energy Reliability . Paper no. TPWRS-00571-2014.

Z. Wang is with the School of Electrical and Computer Engineering, Georgia Institute of Technology, Atlanta, GA 30332 USA (e-mail: zhaoyuwang@gatech.edu).

J. Wang is with the Argonne National Laboratory, Lemont, IL 60439 USA (e-mail: jianhui.wang@anl.gov).

Color versions of one or more of the figures in this paper are available online at http://ieeexplore.ieee.org.

Digital Object Identifier 10.1109/TPWRS.2015.2389753

C. Parameters

G_{ij}	Line conductance between bus i and j.
B_{ij}	Line susceptance between bus i and j.
P_i^D/q_i^D	Active/reactive demand at node i.
V_n	Nominal voltage.
S_{base}	Power base for the system.
$p_{i,n,t}^R$	Predicted active power output of a RES-based DG at node i at time $t, n \in N$.
S_i^G	Capacity of the inverter/converter at node i.
ϵ	Maximum allowed voltage deviation.
γ_s	Probability of sth scenario.
c^G	Generation cost of an MT ($/kW).
$c^{\Delta G}$	Redispatch cost of an MT ($/kW).
c^{emi}	Emission cost of an MT ($/kg).
σ_i	Emission factor of an MT (kg/kWh).
c^D	Price for selling electricity to consumers ($/kWh).
c^S/c^B	Price for selling/buying electricity to/from the upstream system ($/kWh).
π_c/π_d	Charging/discharging efficiency of ES.
EC	Capacity of energy storage.
$\Delta P_{i,s,n,t}^R$	Prediction error of output of type-n DG at node i in scenario s at time t.
α, β	Shape parameters of beta distribution.
T_p	Optimization horizon.
T	Time interval.
ω_k	Priority index of the load at node k.

D. Variables

$V_{i,t}$	Voltage magnitude at node i at time t.
$\theta_{ij,t}$	Phase difference between $V_{i,t}$ and $V_{j,t}$.
$P_{i,t}/Q_{i,t}$	Active/reactive power flow at bus i at time t.
$p_{i,t}^G/q_{i,t}^G$	Active/reactive power generation at node i at time t.
$P_{i,t}^E$	Active power output of the energy storage at node i at time t.
λ/ϕ	Charging/discharging state of ES.
SOC	State of charge of ES.
η_1/θ_1	Power deficiency/surplus of distribution system operator (DSO).
$C_{i,s,t}^{rd}$	Redispatch cost of the MT at bus i at time t in scenario s.

x_{kj}	Indicator of a boundary line of an MG.
$y_{k,t}$	Connection status of the load at bus i at time t (0-shed,1-connect).
$\Delta(\cdot)_s$	Adjustment of $(\cdot)$ in scenario s.

I. Introduction

THE automation of a smart distribution system provides optimal control in the normal operation condition and fast-responding self-healing capability to restore service during an outage. Optimal energy management and self-healing are important features of a smart distribution system. Since the self-healing task is usually performed under emergency conditions after faults, the operational and time constraints can add to the complexity of the problem [1], [2]. With the ever-increasing penetration levels of distributed generators (DGs), the stochasticity of nondispatchable DGs and loads brings new challenges to the operation and self-healing of distribution systems.

Many studies have been made in the literature on the intelligent energy management of a distribution system with DGs. The study in [3]proposed a multi-agent system (MAS)-based scheme for the optimal dispatch of DGs to improve the voltage profile of a distribution system. The study in [4] proposed a power management method by classifying the DGs into utility-owned DGs and independent power producer-owned ones. The study in [5] presented an MAS-based energy management system (EMS) to optimally control DGs in a distribution system so as to guarantee the power balance as well as to optimize the system's efficiency and economy. The study in [6] developed a model predictive control (MPC)-based strategy to regulate the active and reactive power of DGs to improve the voltage and frequency profiles in a distribution system. While the power supply to the consumers may largely rely on DGs after the utility connection fails during an outage, the stochasticity of load consumptions and outputs of nondispatchable DGs are not fully considered in these papers. The study in [7] proposed a stochastic approach to minimize the operation cost of an islanded microgrid (MG). The uncertainty of loads and DG outputs are considered in a scenario-based way. The study in [8] investigated the impacts of various uncertainties on the economical operation of an MG. The study in [9] proposed a scenario tree-based method for matching stochastic supply and demand with optimal control of energy storage systems and minimal wind curtailment and load shedding. The control and power management methods proposed in [3]–[9] are designed for the normal operation condition without considering the self-healing capability of a DG-integrated distribution system.

Self-healing refers to the capability of autonomous service restoration after faults [1]. As an important feature of a smart grid, self-healing has also been studied in the existing literature. The study in [10] proposed an agent-based paradigm for the self-healing protection system with a graph theory-based expert system. The study in [11] introduced a quantitative decision-making model for the distribution system restoration by ranking restoration plans with their performance indices. The intermittency of nondispatchable DGs introduces new challenges to the self-healing control. According to the IEEE Standard 1547.4, splitting a distribution system into multiple MGs can improve the operation and reliability of the distribution network. There are some papers on MG-aided service restoration and optimal operation. The study in [12] discussed the actions and conditions for using MGs for blackstart. The study in [2] proposed the planning framework for an optimal self-healing strategy. However, the optimal energy management of DGs in the normal operation condition is not considered. Moreover, the whole faulted zone is isolated, which increases the unnecessary load shedding. The study in [13] presented self-adequate MG construction plans to make distribution systems more resistant to faults so as to increase reliabilities. The study in [14] combined the load dispatch and network reconfiguration to minimize the operation cost. A bio-inspired algorithm was adopted to solve the problem. However, the paper focuses more on economic operation instead of service restoration. Also, the uncertainties introduced by the intermittent DG outputs and load consumptions make it more difficult to realize optimal energy management and self-healing of a distribution system. It can be seen that the stochastic nature of loads and nondispatchable DGs as well as the optimal operation and self-healing of a DG-integrated distribution system, which are critical features of future smart grids, have not been considered simultaneously in the above existing literature.

In this paper, we present a comprehensive framework for the optimal operation and self-healing of a distribution system. There are two modes of the proposed framework: the normal operation mode and the self-healing mode. In the normal operation mode, the operation costs of the distribution system are minimized by the optimal dispatch of the controllable DGs. The system enters the self-healing mode when there exists a fault/ faults. The on-outage area will be optimally sectionalized into networked self-adequate MGs which can autonomously provide reliable power supply to a maximum number of affected customers. Here, the notion of networked MGs means there are multiple MGs connected with each other and with the distribution system, which can improve the operation and reliability of the system [15], [16]. Self-adequacy refers to generation-load balance within an MG. The controllable DGs in an area that is not affected by the fault (defined as the unfaulted area in this paper) and the sectionalized MGs will be redispatched accordingly. It is assumed that the distribution system consists of dispatchable DGs such as micro turbines (MTs) and nondispatchable DGs such as wind turbines (WTs) and photovoltaic generators (PVs). The model takes into account the uncertainties of nondispatchable DG outputs by applying a stochastic rolling-horizon optimization concept [17], [18]. Load variations are modeled by a normal distribution. The problems are formulated as two-stage stochastic optimization problems. The uncertain load consumptions and power outputs of WTs and PVs are described by scenarios generated from Monte Carlo simulations. The simultaneous backward scenario reduction method [19] is applied to increase the calculation speed while maintaining the accuracy of the solution.

The remainder of this paper is organized as follows. Section II presents the proposed self-healing strategy, the concepts of the rolling-horizon optimization and the associated uncertainties. Section III proposes the stochastic formulations of the optimal normal operation and the self-healing

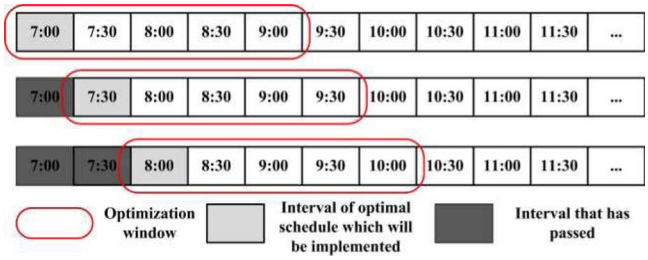

Fig. 1. Demonstration of rolling-horizon optimization [18].

problems. In Section IV, the numerical results are provided. Section V concludes the paper with the major findings.

II. Optimal Self-Healing Strategy

A. Rolling-Horizon Optimization

In analogy to MPC [20], [21], a rolling-horizon optimization is employed to make optimal operation decisions [17], [18]. Fig. 1 is an illustration of the rolling-horizon optimization. An optimization problem is formulated and solved to obtain optimal decisions over the optimization window. However, only the decision for the first time interval in the window is implemented in practice. The solutions for other time intervals will be discarded. The above process is repeated. It is assumed that a prediction algorithm generates estimated load consumption and DG outputs. The prediction technique is beyond the scope of the present paper. In practice, the prediction errors should be considered. The details on prediction errors will be discussed in the Section II-C.

B. Strategy Concept

The proposed control strategy for a distribution system covers the normal operation condition and the emergency reaction after the fault as shown in Fig. 2.

In the normal operation mode, the load demand can always be met. Hence, the operation objectives of the distribution system are to minimize the operation costs such as the generation cost of the dispatchable DGs and to maximize its profits such as selling electricity to consumers and the upstream grid. The control variables are the outputs of dispatchable DGs, which are scheduled based on forecasted loads and nondispatchable DG generations. In order to deal with the stochasticity of loads and nondispatchable DGs, the stochastic rolling-horizon method discussed in section A will be used. The optimal operation problem is formulated as a two-stage stochastic program with the first level to optimize the base generation based on the forecasted outputs of nondispatchable DGs and load consumptions, and the second level to adjust generation according to the variations of realized nondispatchable DG outputs in scenarios.

When faults occur, the traditional distribution system will enter into an isolation and service restoration process by reconfigurations. For a smart distribution system with various types of DGs, this paper proposes a self-healing strategy by sectionalizing the on-outage area into multiple self-adequate MGs so as to optimally perform corrective actions to restore the system

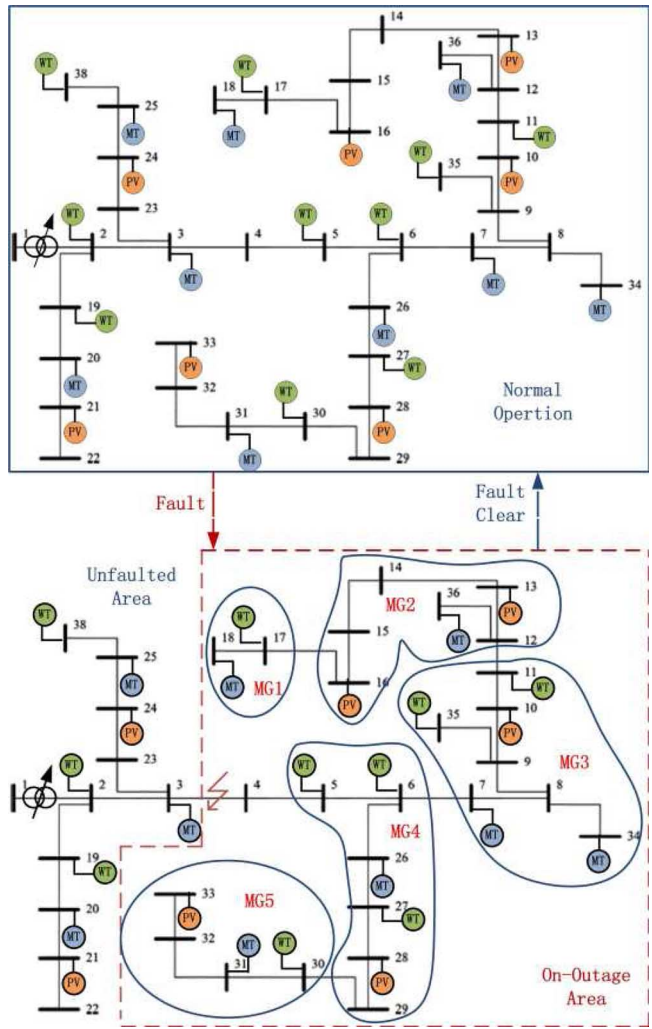

Fig. 2. Concept of the proposed self-healing strategy.

to the best possible stage without violating any operation constraints.

The key point here is to guarantee the supply-demand balance in each MG. To fulfill this goal, two steps are designed. The first step is to sectionalize the on-outage area into networked MGs, adjust the outputs of dispatchable DGs, and perform the necessary load shedding. The objective of the first step is to construct self-supplied MGs and provide reliable power supply to as many customers as possible. The decisions are made based on the forecasts during the fault clearance period (say one to two hours) to make sure the solutions are feasible for all possible scenarios. The second step is to redispatch the controllable DGs in the unfaulted area since the demand and generation conditions have been changed due to the fault. In this paper, it is assumed that the locations of the faults have already been identified. We assume the self-healing process can be smoothly performed, without dynamic and transient stability issues as shown in [1], [14], and [22]. We assume that there is a central controller that can make decisions on network sectionalizing and DG dispatch. The system will go back to the normal operation mode after all faults are cleared and continuously check whether there is a fault. Fig. 3 demonstrates the procedures of the proposed

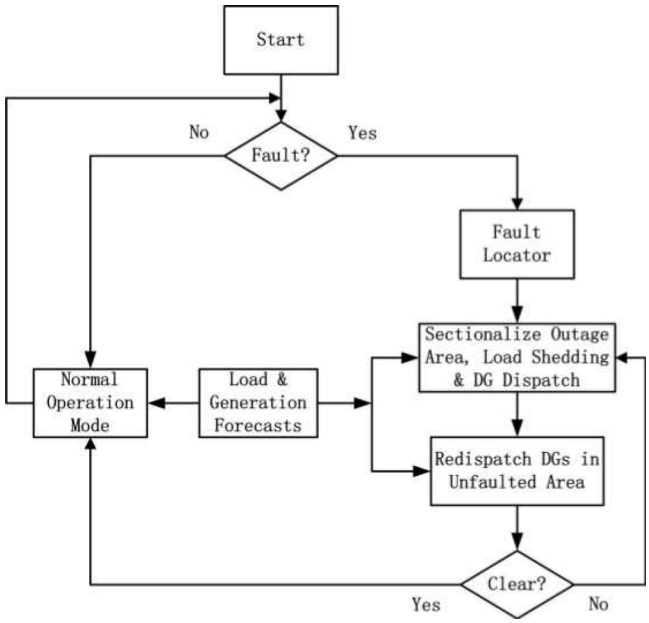

Fig. 3. Flowchart of the proposed operation and self-healing strategy.

comprehensive operation and self-healing strategy. Compared to traditional reconfigurations, sectionalizing the on-outage area into networked MGs has several expected benefits. It can reduce the number and time of actions in the self-healing process since each MG is constructed with the maximum self-adequacy. The sectionalized networked MGs can operate autonomously with the minimum amount of load shedding. The proposed method can improve the reliability of the system operation. It has been shown that cascading faults happen frequently in an extreme weather, e.g., more than 5 times per day during an ice storm [23]. The self-adequate networked MGs formed in the proposed strategy are more resilient to possible cascading faults as the power balance is met locally and those networked MGs can support each other. It is of note that the actual proof of the above expected benefits is still outstanding.

C. Uncertainties and Scenario Reduction

In this paper, two kinds of nondispatchable DGs are considered: WTs and PVs. The predicted load consumptions, wind and solar power will be used. It is known that errors always exist in prediction models. The beta function is shown to be an appropriate distribution to represent prediction errors of wind and solar power [24], [25]. For a predicted power level P_i^R of the DG at node i, the beta function can be defined by two corresponding parameters α and β [24]:

$$f(x) = x^{\alpha-1}(1-x)^{\beta-1}. \tag{1}$$

The above beta function models the occurrence of real power values x when a certain prediction value P_i^R has been forecasted. The shape parameters of the corresponding beta function α and β can be calculated as [24]

$$\frac{P_i^R}{S_{base}} = \frac{\alpha_i}{(\alpha_i+\beta_i)} \tag{2}$$

$$\sigma_i^2 = \alpha_i\beta_i(\alpha_i+\beta_i)^2(\alpha_i+\beta_i+1). \tag{3}$$

The relationship between the predicted power and its error variance can be represented as [24], [26]

$$\sigma_i = \frac{0.2 \times P_i^R}{P_i^{\max} + 0.21}. \tag{4}$$

Using the predicted DG outputs and the (1)–(4), the parameters of beta functions for the current prediction data can be calculated. Meanwhile, the normal distribution is used in this paper to represent the load forecasting errors [27]. Monte Carlo simulation (MCs) is run based on the forecasted power and uncertain prediction errors to generate scenarios for DG outputs. In order to reduce the computation efforts, the simultaneous backward reduction method [19]is implemented to reduce the number of scenarios while maintaining a good approximation of the system uncertainty.

III. Problem Formulation

This section provides the optimization formulations for the normal operation mode and the self-healing mode.

A. Optimization Problem for Normal Operation

The main objectives in the normal operation are to minimize the operation costs and maximize the profits. In this paper, WTs and PVs are considered as nondispatchable DGs, while MTs are considered as dispatchable DGs. The general optimization problem of a distribution system with DGs in the normal operation mode can be formulated as follows:

$$\begin{aligned}\min \sum_{t}^{t+T_p}\Big(&\sum_i c^G p_{i,t}^G + \sum_i c^{emi}\sigma_i p_{i,t}^G - \sum_i c^D p_{i,t}^D + \\ &(c^B\eta_{1,t} - c^S\mu_{1,t}) + \sum_s \gamma_s \sum_i (C_{i,s,t}^{rd} - c^D\Delta p_{i,s,t}^D) \\ &+ \sum_s \gamma_s \sum_i c^{emi}\sigma_i \Delta p_{i,t}^G \\ &+ \sum_s \gamma_s (c^B\Delta\eta_{1,s,t} - c^S\Delta\mu_{1,s,t})\end{aligned} \tag{5}$$

$$\text{s.t. } P_{1,t} = \eta_{1,t} - \mu_{1,t}, \eta, \mu \geq 0, \ \forall t \tag{6}$$

$$1-\epsilon \leq V_{i,t} \leq 1+\epsilon, \forall i \in I, t \tag{7}$$

$$(p_{i,t}^G)^2 + (q_{i,t}^G)^2 \leq S_i^G, \forall i \in I, t \tag{8}$$

$$-P_i^{ch,\max}\lambda_{i,t} \leq p_{i,t}^E \leq P_i^{dch,\max}\phi_{i,t}, \forall i \in I, t \tag{9}$$

$$\lambda_{i,t} + \phi_{i,t} \leq 1, \forall i \in I, t \tag{10}$$

$$\begin{aligned}SOC_{i,t} = SOC_{i,t-1} - \frac{T}{EC_i}&(\phi_{i,t}p_{i,t}^E\pi_d^{-1} \\ &+ \lambda_{i,t}p_{i,t}^E\pi_c), \forall i \in I, t\end{aligned} \tag{11}$$

$$0 \leq SOC_{i,t} \leq SOC_i^{\max}, \forall i \in I, t \tag{12}$$

$$\begin{aligned}P_{i,t} = V_{i,t}\sum_j V_{j,t}(G_{ij}\cos\theta_{ij,t} + B_{ij}\sin\theta_{ij,t}), \\ \forall i \in I, t\end{aligned} \tag{13}$$

$$\begin{aligned}Q_{i,t} = V_{i,t}\sum_j V_{j,t}(G_{ij}\sin\theta_{ij,t} - B_{ij}\cos\theta_{ij,t}), \\ \forall i \in I, t\end{aligned} \tag{14}$$

$$P_{i,t} = p_{i,t}^G + p_{i,t}^E - p_{i,t}^D + \sum_{n\in N} p_{i,n,t}^R, \forall i \in I, t \tag{15}$$

$$Q_{i,t} = q^G_{i,t} - q^D_{i,t} + \sum_{n\in N} q^R_{i,n,t}, \forall i \in I, t \tag{16}$$

$$\sum_i (p^G_{i,t} + p^E_{i,t} + \sum_n p^R_{i,n,t}) \geq \sum_i p^D_{i,t}, \forall t \tag{17}$$

$$\Delta P_{1,s,t} = \Delta\eta_{1,s,t} - \Delta\mu_{1,s,t}, \forall i \in I, s, t \tag{18}$$

$$1 - \epsilon \leq V_{i,t} + \Delta V_{i,t} \leq 1 + \epsilon, \forall i \in I, s, t \tag{19}$$

$$(p^G_{i,t} + \Delta p_{i,s,t})^2 + (q^G_{i,t} + \Delta q^G_{i,s,t})^2 \leq S^G_i, \quad \forall i \in I, s, t \tag{20}$$

$$-P^{ch,\max}_i \lambda_{i,t} \leq p^E_{i,t} + \Delta p^E_{i,s,t} \leq P^{dch,\max}_i \phi_{i,t}, \quad \forall i \in I, s, t \tag{21}$$

$$\Delta SOC_{i,s,t} = \Delta SOC_{i,s,t-1} - \frac{T}{EC_i}(\phi_{i,t}\Delta p^E_{i,s,t}\pi_d^{-1} + \lambda_{i,t}\Delta p^E_{i,s,t}\pi_c), \forall i \in I, s, t \tag{22}$$

$$0 \leq SOC_{i,t} + \Delta SOC_{i,s,t} \leq SOC^{\max}_i, \quad \forall i \in I, s, t \tag{23}$$

$$\Delta P_{i,s,t} = \Delta V_{i,s,t} \sum_j \Delta V_{j,s,t}(G_{ij}\cos(\theta_{ij,t} + \Delta\theta_{ij,s,t}) + B_{ij}\sin(\theta_{ij,t} + \Delta\theta_{ij,s,t})), \forall i \in I, s, t \tag{24}$$

$$\Delta Q_{i,s,t} = \Delta V_{i,s,t} \sum_j \Delta V_{j,s,t}(G_{ij}\sin(\theta_{ij,t} + \Delta\theta_{ij,s,t}) - B_{ij}\cos(\theta_{ij,t} + \Delta\theta_{ij,s,t})), \forall i \in I, s, t \tag{25}$$

$$\Delta P_{i,s,t} = \Delta p^G_{i,s,t} + \Delta p^E_{i,s,t} - \Delta p^D_{i,s,t} + \sum_{n\in N} \Delta p^R_{i,n,s,t}, \forall i \in I, s, t \tag{26}$$

$$\Delta Q_{i,s,t} = \Delta q^G_{i,s,t} - \Delta q^D_{i,s,t} + \sum_{n\in N} \Delta q^R_{i,n,s,t}, \quad \forall i \in I, s, t \tag{27}$$

$$\sum_i (\Delta p^G_{i,s,t} + \Delta p^E_{i,s,t} + \sum_n \Delta p^R_{i,n,s,t}) \geq \sum_i \Delta p^D_{i,s,t}, \forall s, t \tag{28}$$

$$C^{rd}_{i,s,t} \geq c^{\Delta G}\Delta p^G_{i,s,t}, \forall i \in I, s, t \tag{29}$$

$$C^{rd}_{i,s,t} \geq -c^{\Delta G}\Delta p^G_{i,s,t}, \forall i \in I, s, t. \tag{30}$$

In the above formulation, the objective function (5) minimizes the operation costs of the distribution system during the prediction horizon. The objective function can be divided into two parts: the first five items represent the operation costs relative to the base generation schedule made based on the forecasts of load consumptions and the outputs of the nondispatchable DGs. The first item in (5) represents the generation costs of all MTs in the distribution system. The operation costs of RES-based DGs (WTs and PVs in this paper) are not included in the objective function since they have zero fuel cost. The second item in (5) represents the emission cost of MTs. The third item in (5) describes the revenue of selling electricity to customers within the distribution system. The fourth and fifth items in (5) represent the costs of power exchange between the distribution system and the connected upstream network. Buying electricity from the upstream system is considered as positive cost, while selling electricity to the upstream system is considered as negative cost.

However, the nondispatchable DG and loads are uncertain in nature. Hence, the outputs of dispatchable DGs should be adjusted according to the realized scenarios of nondispatchable DG outputs and load consumptions. The last five items in (5) represent the adjustments of the operation costs. The costs include the generation cost of dispatchable DGs (MTs in this paper), and the costs of buying electricity from the connected upstream system.

Constraint (6) represents the power exchange between the distribution system and the upstream system (i.e., if $\eta \geq 0, \mu = 0$ the distribution system is buying electricity from the upstream grid). Constraint (7) guarantees that the voltage level of each node is within a predefined range, ϵ is usually set to be 0.05. Constraint (8) guarantees the output of an inverter/converter is within its capacity. Constraint (9) represents the charging/discharging limits of an energy storage (ES) depending on its operation mode. For example, $x = 1, y = 0$ represents the discharging mode of the ES and the maximum discharging limits are imposed. Constraint (10) guarantees that the ES works in only one mode at a certain time. Constraint (11) represents the state of charge (SOC) of the ES. Constraint (12) represents the limit of SOC. Constraints (13)–(16) are power flow equations. Constraint (17) describes that the total generation should be equal to or larger than the total load consumption. In the formulation (6)–(17), P, Q, V, p^g, q^g, θ, λ, ϕ, SOC, η and μ are the first-stage variables determined based on the forecasts. Since WTs and PVs are non-dispatchable, a forecast is usually used for scheduling purposes. In this paper, the stochastic nature of prediction errors of wind power, solar power and load consumptions is considered as random variables with certain distributions, e.g., the normal distribution and beta distribution are used by previous papers to represent the prediction errors [25], [26], [28]. The second-stage variables should be adjustable in order to deal with the variations of loads and nondispatchable generations [29], [30].

Constraints (18)–(30) describe the second-stage variables Δp, ΔQ, ΔV, Δp^g, Δq^g, $\Delta\theta$, ΔSOC, $\Delta\eta$ and $\Delta\mu$ which are adjusted with the realization of scenarios. Constraint (18) represents the adjustable power exchange between the distribution system and upstream grid in the sth scenario. Constraint (19) guarantees the voltage level at each node is within the permissible range after the generation is adjusted. Constraint (20) guarantees the power output of each inverter/converter is within the permissible range after the generation is adjusted. Constraints (21)–(23) are second-stage constraints for an ES. Constraints (24)–(27) are the adjustable power flow equations for the sth scenario. Constraint (28) describes that the total generation should be equal to or larger than the total load. Constraints (29) and (30) describe the redispatch costs which represent the generation adjustment between the base generation and the generation in the realized scenarios. We can guarantee the redispatch cost of an MT is positive by representing it in the form of constraints (29) and (30) [e.g., if $\Delta p^G_{i,s} \geq 0$, which indicates a generation increase, constraint (30) becomes redundant and the redispatch cost $C^{rd}_{i,s}$ becomes equal to $c^{\Delta G}\Delta p^G_{i,s}$].

B. Optimization Problem for Self-Healing

When a fault or multiple faults happen, the system enters the self-healing stage. In the self-healing mode, the on-outage area will be sectionalized into the networked MGs, the dispatchable DGs in the unfaulted area will be redispatched according to the formulation in (5)–(30) since the load and generation conditions have been changed. For the on-outage area, the highest priority is to maintain a reliable power supply to the affected customers instead of earning economic benefits. The optimization problem for the on-outage area can be formulated as follows:

$$\min \sum_{t}^{t+T_p}(\sum_{s}\gamma_s\sum_{k}(|V_{k,s,t}-V_n|+\sum_{j}x_{kj} +\omega_k p^D_{k,s,t}(1-y_{k,t}))) \quad (31)$$

$$\text{s.t. } 1-\epsilon \le V_{k,s,t} \le 1+\epsilon, \forall k,s,t \quad (32)$$

$$p^G_{k,s,t}-y_{k,t}p^D_{k,s,t}+\sum_{n\in N}p^R_{k,n,s,t}=\sum_j P_{kj,s,t}, \quad \forall k,s,t \quad (33)$$

$$q^G_{k,s,t}-y_{k,t}q^D_{k,s,t}+\sum_{n\in N}q^R_{k,n,s,t}=\sum_j Q_{kj,s,t}, \quad \forall k,s,t \quad (34)$$

$$P_{kj,s,t}=x_{kj}V_{k,s,t}V_{j,s,t}(G_{kj}\cos\theta_{kj,s,t} + B_{kj}\sin\theta_{kj,s,t}), \forall k,s,t \quad (35)$$

$$Q_{kj,s,t}=x_{kj}V_{k,s,t}V_{j,s,t}(G_{kj}\sin\theta_{kj,s,t} - B_{kj}\cos\theta_{kj,s,t}), \forall k,s,t \quad (36)$$

$$(p^G_{k,s,t})^2+(q^G_{k,s,t})^2 \le S^G_k, \forall k,s,t \quad (37)$$

$$-P^{ch,\max}_k\lambda_{k,t} \le p^E_{k,s,t} \le P^{dch,\max}_k\phi_{k,t}, \quad \forall k,s,t \quad (38)$$

$$\lambda_{k,t}+\phi_{k,t}\le 1, \forall k,t \quad (39)$$

$$SOC_{k,s,t}=SOC_{k,s,t-1}-\frac{T}{EC_k}(\phi_{k,t}p^E_{k,s,t}\pi_d^{-1} + \lambda_{k,t}p^E_{k,s,t}\pi_c), \forall k,s,t \quad (40)$$

$$0\le SOC_{k,s,t}\le SOC^{\max}_k, \forall k,s,t \quad (41)$$

$$\sum_k(p^G_{k,s,t}+p^E_{k,s,t}+\sum_n p^R_{k,n,s,t}) \ge \sum_k p^D_{k,s,t}, \forall s,t \quad (42)$$

$$\sum_k(q^G_{k,s,t}+\sum_n q^R_{k,n,s,t}) \ge \sum_k q^D_{k,s,t}, \forall k,s,t. \quad (43)$$

The objective function (31) is to optimally partition the on-outage area into networked MGs based on the forecasted load consumptions and DG outputs so that the maximum load within each MG can be supplied with reliable power generation. The first item in (31) represents the voltage deviations from the nominal voltage. The second and third items in (31) describe the power flow in the lines of each MG. $x_{kj}=0$ means the line between the buses k and j is a candidate of boundary lines between two self-adequate MGs with minimized generation-load imbalance. In other words, $x_{kj}=0$ does not mean the line will be cut, but means the power flow on the line could be zero without affecting the operation of the MGs. The last item in (31) is the penalty function for load shedding according to their importance. Constraint (32) guarantees that the voltage level of each node is within a permissible range. Constraints (33)–(36) are the power flow equations. Constraint (37) describes the output of an inverter/converter should be within its capacity. Constraints (38)–(41) are for energy storage systems. In constraints (42) and (43), the total generation should be equal to or larger than the total load in all scenarios. The control variables are the boundary line indicator x_{kj}, the outputs of dispatchable DGs p^G_k and the load shedding indicator y_k.

In sum, the problem formulated in (5)–(30) is for the normal operation mode and the problem formulated in (31)–(43) is for the self-healing mode. Both are mix-integer non-linear programming (MINLP) problems and can be solved by commercial solvers, such as DICOPT [31].

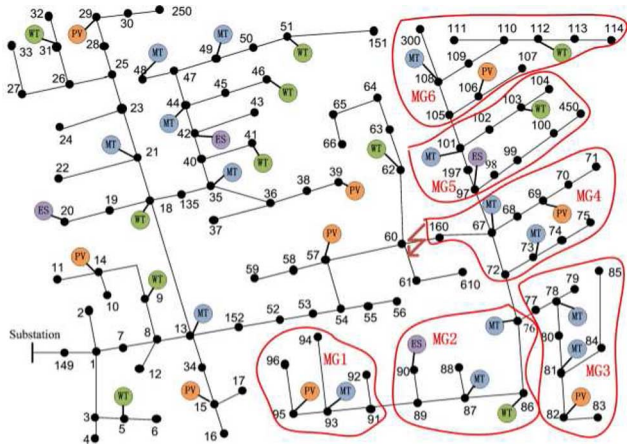

Fig. 4. Modified IEEE 123-bus test system.

IV. Numerical Results

The proposed method has been examined on a modified IEEE 123-bus distribution system as shown in Fig. 4. Details about the test system can be found in [32]. Table I summarizes the types, locations and capacities of the DGs integrated in the system. Table II shows the parameters used in the case study, which are obtained from [33]. All the costs and electricity prices are presented in U.S. dollars. It is assumed that the predicted loads and nondispatchable DG outputs are products of the basic components and the multipliers. The values of basic load components can be found in [32]. The basic components for DGs are assumed to be the corresponding capacities. The assumed multipliers, as shown in Figs. 5 and 6, are used to make the load profiles and predicted DG outputs change with time. For illustration, we assume that the multipliers of all nodes are the same. In practice, loads and DG outputs at different nodes may change with different profiles. The proposed method can still be applied by assigning various profiles to different nodes. The operator can change the multipliers according to the available system information. The probabilistic distributions of forecast errors can be estimated using the method described in Section III-C.

For illustration, we set the prediction horizon to be 2 h and the time step to be 30 min. The operators can change these settings according to their preference and operation conditions.

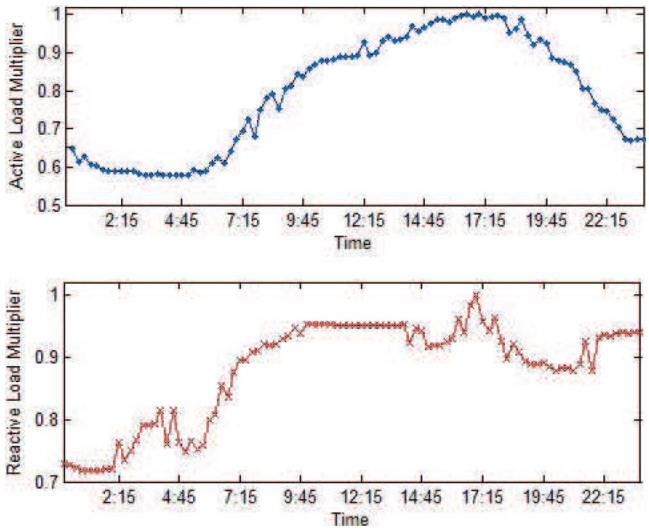

Fig. 5. Load profile multipliers.

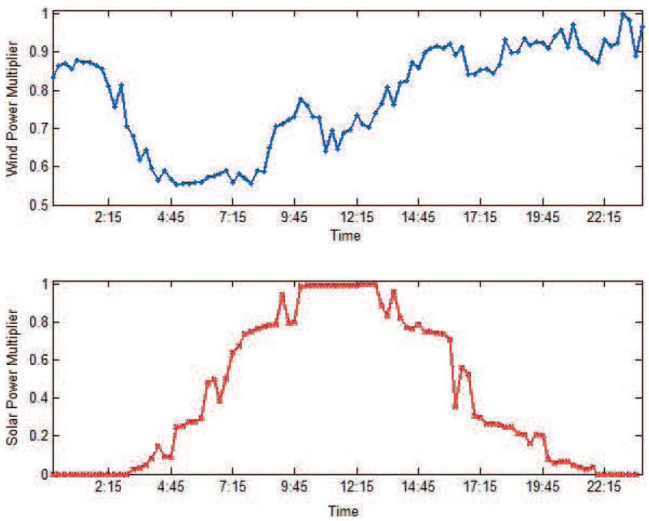

Fig. 6. Predicted wind and solar power multipliers.

TABLE I
LOCATIONS AND SIZES OF DGS

Type	Locations(Node No.)	Sizes(kW)
WT	5, 9, 18, 31, 41, 46, 51, 62, 86, 103, 112	80, 60, 100, 80, 30, 80, 95, 60, 100, 85, 50, 50, 60
PV	14, 15, 29, 39, 57, 69, 82, 95, 106	60, 60, 60, 80, 40, 80, 60, 40, 40, 60
MT	13, 21, 35, 44, 48, 49, 67, 73, 76, 78, 81, 87, 93, 101, 108	80, 180, 120, 140, 100, 160, 110, 140, 140, 120, 80, 140, 100, 150, 160
ES	20, 42, 90, 97	150, 200, 60, 150

TABLE II
PARAMETERS FOR CALCULATING CORRESPONDING COSTS

Parameters		Value	
c^G	\$0.1/kWh	c^D	\$0.3/kWh
$c^{\Delta G}$	\$0.15/kW	$c^S = c^B$	\$0.1/kWh
c^{emi}	\$0.02/kg	σ	0.003 kg/kWh

TABLE III
GENERATION DISPATCHES (kW) OF MTS IN THE NORMAL OPERATION MODE

14:00	Node No.	13	21	35	44	48
	Dispatch	**62**	**131**	**75**	**92**	**107**
	Node No.	49	67	73	76	78
	Dispatch	**120**	**92**	**62**	**121**	**106**
	Node No.	81	87	93	101	108
	Dispatch	**76**	**114**	**83**	**109**	**107**
14:30	Node No.	13	21	35	44	48
	Dispatch	**58**	**120**	**74**	**88**	**103**
	Node No.	49	67	73	76	78
	Dispatch	**117**	**85**	**60**	**115**	**102**
	Node No.	81	87	93	101	108
	Dispatch	**77**	**111**	**80**	**104**	**105**
15:00	Node No.	13	21	35	44	48
	Dispatch	**65**	**97**	**81**	**96**	**112**
	Node No.	49	67	73	76	78
	Dispatch	**127**	**94**	**63**	**125**	**115**
	Node No.	81	87	93	101	108
	Dispatch	**78**	**119**	**87**	**110**	**109**
15:30	Node No.	13	21	35	44	48
	Dispatch	**64**	**96**	**83**	**98**	**115**
	Node No.	49	67	73	76	78
	Dispatch	**131**	**91**	**64**	**129**	**116**
	Node No.	81	87	93	101	108
	Dispatch	**83**	**121**	**89**	**104**	**112**

This means for every 30 min, the system predicts the DG outputs for the next 2 h and makes optimal decisions. The maximum SOC is set to be 0.9 for all ES, the maximum charging/discharging rate is set to be 50% of the ES size, π_d and π_c are set to be 0.95 for all ES. One thousand scenarios are generated using the Monte Carlo simulation to represent the prediction errors in the prediction horizon. As discussed in the previous section, the scenario reduction is applied to reduce the computation efforts while maintaining the solution accuracy. The 1000 generated scenarios are reduced to 15 scenarios in this case. All the above settings are for illustration and can be changed according to the availability of forecasted data.

A. Normal Operation Mode

This case demonstrates how the proposed comprehensive operation and self-healing strategy works in the normal operation mode. The objective in this mode is to maximize the revenues. Based on the forecasted loads and DG outputs as well as the rolling-horizon formulation of (5)–(30), the optimal dispatch of MTs can be achieved. For illustration, the optimal dispatch between 14:00 to 15:30 is shown in Table III. Table IV shows the outputs of ES systems. Table V shows the costs and revenues of the distribution system during this period.

In order to investigate the impacts of various prediction horizons and time steps on the dispatch results, a sensitivity analysis has been performed. The time step is set to be 15, 30, and 45 min; the prediction horizon is set to be 1, 2, and 3 h. For illustration, Table VI shows the generation schedule of MT13 with different time steps and prediction horizons at 14:00.

For the particular problem and data in this paper, it can be seen that the MT output increases as the prediction horizon be-

TABLE IV
ES DISPATCHES (KW) IN THE NORMAL OPERATION MODE

Time	ES Dispatches (kW) in the Normal Operation Mode			
14:00	ES 20	ES 42	ES 90	ES 97
	-18	66	19	41
14:30	ES 20	ES 42	ES 90	ES 97
	-12	70	19	44
15:00	ES 20	ES 42	ES 90	ES 97
	10	72	20	45
15:30	ES 20	ES 42	ES 90	ES 97
	15	74	20	46

Note: Negative dispatch represents charging and positive dispatch represents discharging.

TABLE V
REVENUES AND COSTS (IN US DOLLARS) IN THE NORMAL OPERATION MODE

Time	Revenues	Generation Cost	Loss Cost	Power Exchange Cost
14:00	361.4	72.5	18.8	40.9
14:30	370.7	69.6	15.5	43.6
15:00	377.1	73.9	17.9	41.9
15:30	377.8	75.6	21.2	42.6

TABLE VI
GENERATION DISPATCHES (KW) OF MT13 WITH DIFFERENT TIME STEPS AND PREDICTION HORIZONS AT 14:00

$T_p = 1$ hr	T(min.)	15	30	45
	Dispatch (kW)	**61**	**61**	**62**
$T_p = 2$ hr	T(min.)	15	30	45
	Dispatch (kW)	**62**	**62**	**63**
$T_p = 3$ hr	T(min.)	15	30	45
	Dispatch (kW)	**63**	**64**	**65**

comes longer. The reason is that more uncertainties are involved in the decision-making process with a longer prediction horizon. Thus, the algorithm will make a more conservative decision by increasing the outputs of controllable DGs. Fig. 7 shows the total generation costs with different prediction horizons from 14:00 to 15:30. We assume the time step is 30 min, and the prediction horizons are set to be 1, 2, and 3 h. It can be seen that the generation costs increase as the prediction horizon becomes longer, which is due to the increased MT outputs.

B. Self-Healing Mode for a Single Fault

This case shows the performance of the proposed method in the self-healing mode. It is assumed that a single permanent fault happens in the line 60–160 at 15:30, the fault clearance time is one hour and a half [1]. This means the optimal self-healing strategy should be planned for the time period between 15:30 to 17:00. The objective of the self-healing mode is to optimally sectionalize the on-outage area into the networked MGs and redispatch MTs so as to provide reliable power supply to the affected loads and minimize the load shedding. The optimum system partitioning results are shown in Fig. 4. The on-outage area has been sectionalized into six MGs which are named as MG1 to MG6.

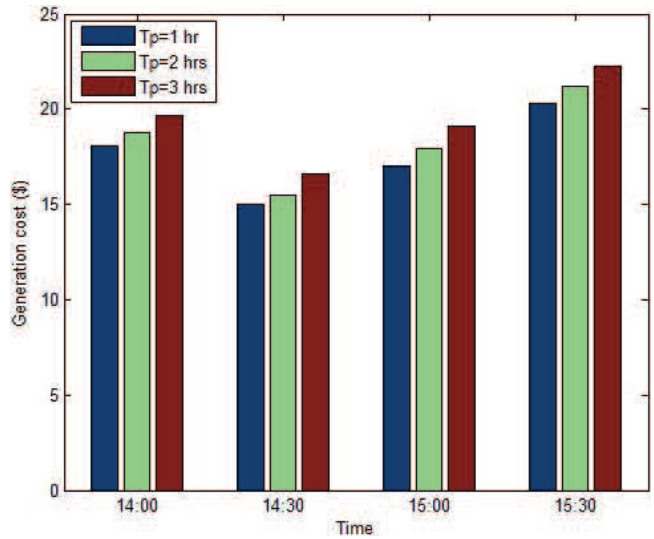

Fig. 7. Generation costs with different prediction horizons.

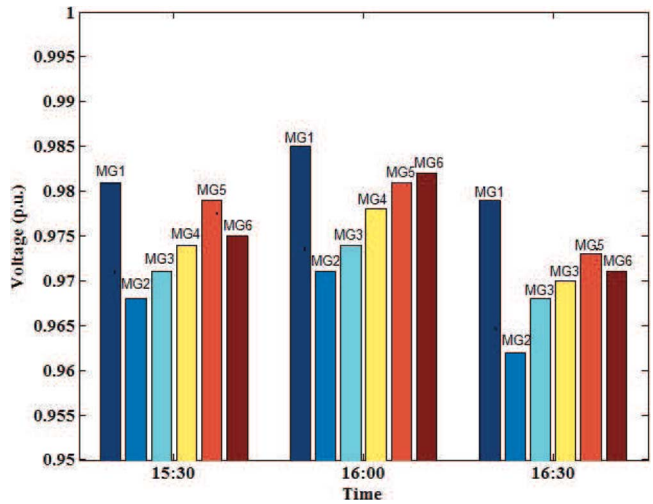

Fig. 8. Lowest voltage level in each MG in a single fault (Case B).

Table VII shows the generation dispatches of MTs and the load shedding in each MG in a single fault (Case B). Since the power balance within each MG is critical, it can be seen that MG1, MG3, MG5, and MG6 are self-adequate without any load shedding while MG2 and MG4 become self-sufficient through the minimum load shedding (node 70). The ES dispatches are shown in Table VIII. It can be seen that all ESs are working in the discharging mode to guarantee the generation-demand balance within each MG. The security and stability of the networked MGs is another major concern in the self-healing strategy. Fig. 8 shows the lowest voltage of each MG during the fault clearance period. It can be seen that the lowest voltage levels are always within the safe range $(\pm 5\%)$ [34]. The highest recorded voltage in the simulation is 1.01 p.u. which is also within the safe range.

Since the load and generation conditions are changed due to the fault, it is necessary to redispatch the MTs in the unfaulted area for the optimal operation. The operational goal of the unfaulted area is still to maximize the profit. Table IX shows the redispatch results. Take the dispatch at 15:30 as an example, the

TABLE VII
GENERATION DISPATCHES (kW) AND LOAD SHEDDING (NODE NUMBER) IN THE SELF-HEALING MODE FOR CASE B

Time	MG#	MT (Node#)	Schedule (kW)	Load Shed (Node #)	Load Shed (kW)
15:30	MG1	MT 93	88	N/A	N/A
	MG2	MT 76	151	N/A	N/A
		MT 87	143		
	MG3	MT 78	120	N/A	N/A
		MT 81	92		
	MG4	MT 67	104	70	20
		MT 73	72		
	MG5	MT 101	122	N/A	N/A
	MG6	MT 108	123	N/A	N/A
16:00	MG1	MT 93	90	N/A	N/A
	MG2	MT 76	145	N/A	N/A
		MT 87	139		
	MG3	MT 78	118	N/A	N/A
		MT 81	91		
	MG4	MT 67	107	70	20
		MT 73	75		
	MG5	MT 101	124	N/A	N/A
	MG6	MT 108	117	N/A	N/A
16:30	MG1	MT 93	98	N/A	N/A
	MG2	MT 76	152	N/A	N/A
		MT 87	144		
	MG3	MT 78	128	N/A	N/A
		MT 81	92		
	MG4	MT 67	114	70	20
		MT 73	76		
	MG5	MT 101	129	N/A	N/A
	MG6	MT 108	130	N/A	N/A

Note: The number after MT represents the installation bus, e.g., MT 93 represents the MT at bus 93.

TABLE VIII
ES DISPATCHES (kW) IN THE SELF-HEALING MODE FOR CASE B

Time	ES (Node #) & Dispatch (kW)			
15:30	ES 20	ES 42	ES 90	ES 97
	45	73	21	46
16:00	ES 20	ES 42	ES 90	ES 97
	43	74	21	47
16:30	ES 20	ES 42	ES 90	ES 97
	34	73	20	46

Note: Negative dispatch represents charging and positive dispatch represents discharging.

TABLE IX
GENERATION DISPATCHES (kW) OF MTS IN THE UNFAULTED AREA

Time	MT 13	MT 21	MT 35	MT 44	MT 48	MT 49
15:30	55	57	68	84	95	109
16:00	62	61	77	92	109	118
16:30	74	75	90	116	128	143

MT outputs in Table IX are smaller than those in Table III. This is because parts of the loads are supplied by the networked MGs.

C. Self-Healing Mode for Multiple Faults

This case tests the performance of the proposed method with multiple simultaneous faults. It is assumed that two permanent faults happen in the system, one is in the line 18–135 and the other is in the line 60–160 at 15:30, the fault clearance time is one hour and a half. The optimum system partitioning results are shown in Fig. 9. The on-outage area has been sectionalized into nine MGs which are named as MG1 to MG9. The redispatch and load shedding results from MG1 to MG6 are the same as shown in Table VI. The results for MG 7 to MG9 are shown in Table X. Fig. 10 shows the lowest voltage of each MG during the fault clearance period. It can be seen that the lowest voltage levels are within the safe range ($\pm 5\%$).

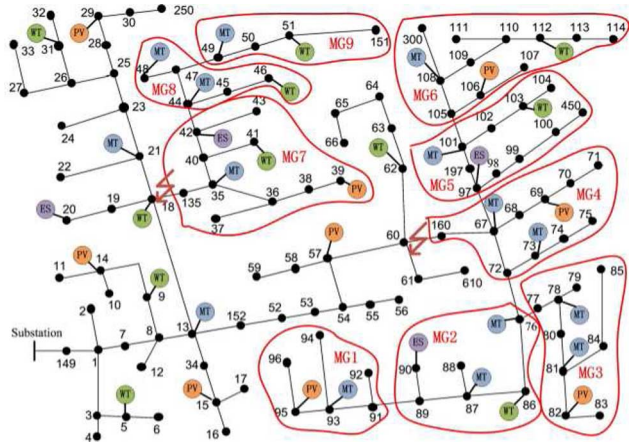

Fig. 9. Modified IEEE 123-bus test system with multiple faults.

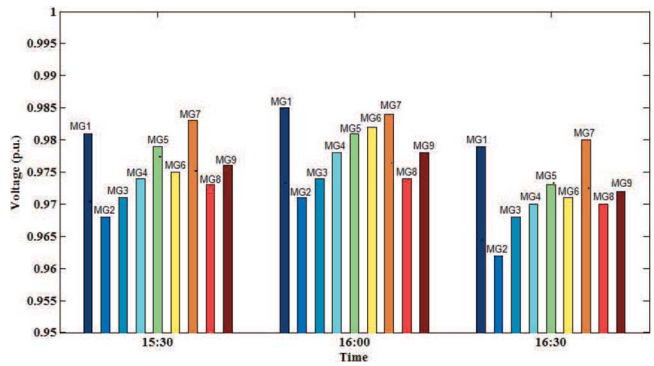

Fig. 10. Lowest voltage level in each MG in multiple faults (Case C).

TABLE X
GENERATION DISPATCHES (kW) AND LOAD SHEDDING (NODE NUMBER) IN THE SELF-HEALING MODE FOR CASE C

Time	MG#	Type (Node#)	Schedule (kW)	Load Shed (Node #)	Load Shed (kW)
15:30	MG7	MT 35	77	N/A	N/A
		ES 42	73		
	MG8	MT 44	110	45	20
		MT 48	131		
	MG9	MT 49	145	N/A	N/A
16:00	MG7	MT 35	76	N/A	N/A
		ES 42	74		
	MG8	MT 44	109	45	20
		MT 48	129		
	MG9	MT 49	142	N/A	N/A
16:30	MG7	MT 35	87	N/A	N/A
		ES 42	73		
	MG8	MT 44	113	45	20
		MT 48	135		
	MG9	MT 49	150	N/A	N/A

In order to demonstrate the advantages of the proposed method over the traditional service restoration methods such as the one introduced in [35]we consider the following example: a fault occurs on line section 60-160 and then a cascading fault occurs on line section 67-72. For the proposed self-healing method based on networked MGs, the on-fault area will be sectionalized into networked MGs as shown in Fig. 4 when the first fault on line 60–160 happened. After a cascading fault happened, the on-fault MG will be further sectionalized and the operation of other MGs will be not affected. However, according to the method in [35], both the tie-switches 151–300 and 54–94 need to be closed in response to the cascading faults. It can be seen that the traditional methods depend on the availability and functionality of tie-switches and it also needs more actions to restore the service.

V. Conclusion

This paper provides a novel methodology for the optimal operation and self-healing of a DG-integrated distribution system. The proposed approach minimizes the operation costs in the normal operation mode and guarantees the reliable power supply to consumers during the faults by: the two-stage stochastic and rolling-horizon formulation to optimize the operation costs and profits by scheduling the outputs of controllable DGs and ESs, the on-outage area is optimally sectionalized into networked self-supplied MGs to provide power supply to the affected customers and increase the operational flexibility and reliability, and the controllable DGs are redispatched accordingly in the sectionalized networked MGs to support the reliable operation as well as in the unfaulted area to maintain its economic operation. The proposed method is the further development and application of networked MGs. Case studies on the modified IEEE 123-bus system show that the proposed comprehensive operation and self-healing technique can assist the construction of a smart and resilient distribution system.

The future research needs include quantifying the resilience of a distribution grid with the proposed self-healing strategy, developing a set of extreme scenarios to determine their effects on distribution grids, designing distribution grids considering self-healing strategies in extreme events, and developing optimal restoration actions by taking advantage of the sectionalized networked MGs.

References

[1] A. Zidan and E. El-Saadany, "A cooperative multiagent framework for self-healing mechanisms in distribution systems," *IEEE Trans. Smart Grid*, vol. 3, no. 3, pp. 1525–1539, Sep. 2012.

[2] S. Arefifar, Y.-R. Mohamed, and T. El-Fouly, "Comprehensive operational planning framework for self-healing control actions in smart distribution grids," *IEEE Trans. Power Syst.*, vol. 28, no. 4, pp. 4192–4200, Nov. 2013.

[3] M. Baran and I. El-Markabi, "A multiagent-based dispatching scheme for distributed generators for voltage support on distribution feeders," *IEEE Trans. Power Syst.*, vol. 22, no. 1, pp. 52–59, Feb. 2007.

[4] S. Lee, G. Son, and J.-W. Park, "Power management and control for grid-connected DGs with intentional islanding operation of inverter," *IEEE Trans. Power Syst.*, vol. 28, no. 2, pp. 1235–1244, May 2013.

[5] F. Ren, M. Zhang, and D. Sutanto, "A multi-agent solution to distribution system management by considering distributed generators," *IEEE Trans. Power Syst.*, vol. 28, no. 2, pp. 1442–1451, May 2013.

[6] M. Falahi, S. Lotfifard, M. Ehsani, and K. Butler-Purry, "Dynamic model predictive-based energy management of DG integrated distribution systems," *IEEE Trans. Power Del.*, vol. 28, no. 4, pp. 2217–2227, Oct. 2013.

[7] A. Sobu and G. Wu, "Optimal operation planning method for isolated micro grid considering uncertainties of renewable power generations and load demand," in *Proc. 2012 IEEE Innovative Smart Grid Technologies—Asia (ISGT Asia)*, May 2012, pp. 1–6.

[8] M. Wang and H. Gooi, "Effect of uncertainty on optimization of microgrids," in *Proc. IPEC 2010 Conf.* , Oct. 2010, pp. 711–716.

[9] J. Wu and X. Guan, "A stochastic matching mechanism for wind generation dispatch and load shedding allocation in microgrid," in *Proc. 2014 IEEE PES Innovative Smart Grid Technologies Conf. (ISGT)*, Feb. 2014, pp. 1–5.

[10] S. Sheng, K. Li, W. Chan, Z. Xiangjun, and D. Xianzhong, "Agent-based self-healing protection system," *IEEE Trans. Power Del.*, vol. 21, no. 2, pp. 610–618, Apr. 2006.

[11] W.-H. Chen, "Quantitative decision-making model for distribution system restoration," *IEEE Trans. Power Syst.*, vol. 25, no. 1, pp. 313–321, Feb. 2010.

[12] C. Moreira, F. Resende, and J. P. Lopes, "Using low voltage microgrids for service restoration," *IEEE Trans. Power Syst.*, vol. 22, no. 1, pp. 395–403, Feb. 2007.

[13] S. Arefifar, Y.-R. Mohamed, and T. EL-Fouly, "Optimum microgrid design for enhancing reliability and supply-security," *IEEE Trans. Smart Grid*, vol. 4, no. 3, pp. 1567–1575, Sep. 2013.

[14] S. Tan, J.-X. Xu, and S. Panda, "Optimization of distribution network incorporating distributed generators: An integrated approach," *IEEE Trans. Power Syst.*, vol. 28, no. 3, pp. 2421–2432, Aug. 2013.

[15] H. K. Nunna and S. Doolla, "Multiagent-based distributed-energy-resource management for intelligent microgrids," *IEEE Trans. Ind. Electron.*, vol. 60, no. 4, pp. 1678–1687, Apr. 2013.

[16] M. Fathi and H. Bevrani, "Adaptive energy consumption scheduling for connected microgrids under demand uncertainty," *IEEE Trans. Power Del.*, vol. 28, no. 3, pp. 1576–1583, Jul. 2013.

[17] P. Malysz, S. Sirouspour, and A. Emadi, "An optimal energy storage control strategy for grid-connected microgrids," *IEEE Trans. Smart Grid*, vol. 5, no. 4, pp. 1785–1796, Jul. 2014.

[18] A. O'Connell, D. Flynn, and A. Keane, "Rolling multi-period optimization to control electric vehicle charging in distribution networks," *IEEE Trans. Power Syst.*, vol. 29, no. 1, pp. 340–348, Jan. 2014.

[19] H. Heitsch and W. R?misch, "Scenario reduction algorithms in stochastic programming," *Computat. Optimiz. Applicat.*, vol. 24, no. 2-3, pp. 187–206, 2003 [Online]. Available: http://dx.doi.org/10.1023/A%3A1021805924152

[20] Z. Wang, J. Wang, B. Chen, M. Begovic, and Y. He, "Mpc-based voltage/var optimization for distribution circuits with distributed generators and exponential load models," *IEEE Trans. Smart Grid*, vol. 5, no. 5, pp. 2412–2420, Sep. 2014.

[21] M. Moradzadeh, R. Boel, and L. Vandevelde, "Anticipating and coordinating voltage control for interconnected power systems," *Energies*, vol. 7, no. 2, pp. 1027–1047, 2014 [Online]. Available: http://www.mdpi.com/1996–1073/7/2/1027

[22] H. Liu, X. Chen, K. Yu, and Y. Hou, "The control and analysis of self-healing urban power grid," *IEEE Trans. Smart Grid*, vol. 3, no. 3, pp. 1119–1129, Sep. 2012.

[23] D. Xianzhong and S. Sheng, "Self-organized criticality in time series of power systems fault, its mechanism, and potential application," *IEEE Trans. Power Syst.*, vol. 25, no. 4, pp. 1857–1864, Nov. 2010.

[24] A. Fabbri, T. Roma?n, J. Abbad, and V. Quezada, "Assessment of the cost associated with wind generation prediction errors in a liberalized electricity market," *IEEE Trans. Power Syst.*, vol. 20, no. 3, pp. 1440–1446, Aug. 2005.

[25] H. Bludszuweit, J. Dominguez-Navarro, and A. Llombart, "Statistical analysis of wind power forecast error," *IEEE Trans. Power Syst.*, vol. 23, no. 3, pp. 983–991, Aug. 2008.

[26] T. Niknam, M. Zare, and J. Aghaei, "Scenario-based multiobjective volt/var control in distribution networks including renewable energy sources," *IEEE Trans. Power Del.*, vol. 27, no. 4, pp. 2004–2019, Oct. 2012.

[27] B.-M. Hodge, D. Lew, and M. Milligan, "Short-term load forecast error distributions and implications for renewable integration studies," in *Proc. 2013 IEEE Green Technologies Conf.*, Apr. 2013, pp. 435–442.

[28] E. Castronuovo and J. P. Lopes, "On the optimization of the daily operation of a wind-hydro power plant," *IEEE Trans. Power Syst.*, vol. 19, no. 3, pp. 1599–1606, Aug. 2004.

[29] R. Jabr, "Adjustable robust OPF with renewable energy sources," *IEEE Trans. Power Syst.*, vol. 28, no. 4, pp. 4742–4751, Nov. 2013.
[30] J. Wang, M. Shahidehpour, and Z. Li, "Security-constrained unit commitment with volatile wind power generation," *IEEE Trans. Power Syst.*, vol. 23, no. 3, pp. 1319–1327, Aug. 2008.
[31] M. R. Bussieck and S. Vigerske, MINLP Solver Software. New York, NY, USA, Wiley, 2010 [Online]. Available: http://dx.doi.org/10.1002/9780470400531.eorms0527
[32] W. Kersting, "Radial distribution test feeders," *IEEE Trans. Power Syst.*, vol. 6, no. 3, pp. 975–985, Aug. 1991.
[33] K. Zou, A. Agalgaonkar, K. Muttaqi, and S. Perera, "Distribution system planning with incorporating DG reactive capability and system uncertainties," *IEEE Trans. Sustain. Energy*, vol. 3, no. 1, pp. 112–123, Jan. 2012.
[34] ANSI C84.1–1995 "ANSI standard for electric power systems and equipment voltage ratings (60 Hz)," May 1995, pp. C1–42.
[35] H. Fan, P. Backscheider, J. Fan, and J. McDonald, "Collaborative optimization of distribution grid operation," in *Proc. 2012 IEEE PES Innovative Smart Grid Technologies (ISGT)*, Jan. 2012, pp. 1–6.

Zhaoyu Wang (S'13) received the B.S. degree in electrical engineering from Shanghai Jiaotong University, Shanghai, China, in 2009, the M.S. degree in electrical engineering from Shanghai Jiaotong University in 2012, and the M.S. degree in electrical and computer engineering from the Georgia Institute of Technology, Atlanta, GA, USA, in 2012. He is now pursuing the Ph.D. degree in the School of Electrical and Computer Engineering, Georgia Institute of Technology.

In 2013, he worked as a research aide intern at Decision and Information Sciences Division, Argonne National Laboratory, Argonne, IL, USA. His current research interests include microgrids, cyber-physical systems, volt/var control, demand response and energy conservation, system modeling and identification, and power system optimization.

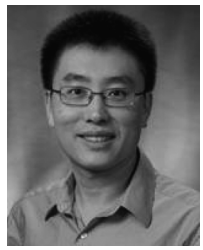

Jianhui Wang (M'07–SM'12) received the Ph.D. degree in electrical engineering from the Illinois Institute of Technology, Chicago, IL, USA, in 2007.

Presently, he is the Section Lead for Advanced Power Grid Modeling at the Energy Systems Division at Argonne National Laboratory, Argonne, IL, USA. He is also an affiliate professor at Auburn University and an adjunct professor at University of Notre Dame.

Dr. Wang is the secretary of the IEEE Power & Energy Society (PES) Power System Operations Committee. He is the Editor-in-Chief of the IEEE TRANSACTIONS ON SMART GRID and an IEEE PES Distinguished Lecturer.